J Solid State Electrochem (2008) 12:1077–1084
DOI 10.1007/s10008-007-0437-7

ORIGINAL PAPER

Solid state electrochemical of the erbium hexacyanoferrate-modified carbon ceramic electrode and its electrocatalytic oxidation of L-cysteine

Qing-Lin Sheng · Hao Yu · Jian-Bin Zheng

Received: 8 July 2007 / Revised: 14 September 2007 / Accepted: 19 September 2007 / Published online: 31 October 2007

Abstract A kind of erbium hexacyanoferrate (ErHCF)-modified carbon ceramic electrodes (CCEs) fabricated by mechanically attaching ErHCF samples to the surface of CCEs derived from sol–gel technique was proposed. The resulting modified electrodes exhibit well-defined redox responses with the formal potential of +0.215 V [vs saturated calomel electrode (SCE)] at a scan rate of 20 mV s^{-1} in 0.5 M KCl (pH 7) solution. The voltammetric characteristics of the ErHCF-modified CCEs were investigated by voltammetry. Attractively, the ErHCF-modified CCEs presented good electrocatalytic activity with a marked decrease in the overvoltage about 400 mV for L-cysteine oxidation. The calibration plot for L-cysteine determination was linear at 5.0×10^{-6}–1.3×10^{-4} M with a linear regression equation of I (A)=0.558+0.148c (μM) (R^2=0.9989, n=20), and the detection limit was 2×10^{-6} M (S/N=3). At last, the ErHCF-modified CCEs were used for amperometric detection of L-cysteine in real samples.

Keywords Erbium hexacyanoferrate · Carbon ceramic electrode · Electrochemical behavior · Electrocatalytic oxidation · L-cysteine

Introduction

In recent years, modification of electrode surfaces with various electroactive materials is an interesting area of research in designing electrochemical sensors. Various organic and inorganic modifiers have been immobilized on conducting substrate electrodes to prepare chemically modified electrodes (CMEs) [1]. Metal hexacyanoferrates (MHCFs), a class of polynuclear mixed-valence compounds, have attracted much attention because of their special properties such as ion-exchange selectivity [2, 3], electrochromism [4–6], solid-state batteries [7–9], photoimage formation [10, 11], magnetism [12], and electrocatalysis [13, 14].

Since the pioneering works on Prussian Blue (PB)-modified electrodes reported by Neff and Itaya [15, 16], PB and its analogues form an important part of electroactive materials in preparation for chemically modified electrodes and chemical sensors. However, much attention has been focused on transition MHCFs to fabricate different kinds of modified electrodes for electroanalytical studies [17–22]. In recent years, rare earth MHCFs have received much attention in many fields because of their special properties and potential applications [23–27], such as the hydrogen storage materials of batteries [28], electrocatalytic hydrogenation of alkenes [29], and chemical sensors [30]. Furthermore, the study of the electrochemistry of solid hexacyanoferrates is very important to gain access to the fundamentals of solid-state electrochemistry [31]. Liu and Chen [32] have reported lanthanum hexacyanoferrate (LaHCF)-modified electrode by electrochemical scanning at a platinum electrode and characterized the electrode with various techniques. The electrochemical characteristics of the dysprosium hexacyanoferrate (DyHCF) were studied by solid-state electrochemistry [33]. After that, Cai et al. reported the electrochemical properties of LaHCF [34], DyHCF [35], and samarium hexacyanoferrate (SmHCF) [36] by using the method developed by Scholz and coworkers [37, 38]. They also studied the electrocatalytic activities of SmHCF toward dopamine [39] and the effects

Q.-L. Sheng · H. Yu · J.-B. Zheng (✉)
Institute of Analytical Science/Shaanxi Provincial Key Lab of Electroanalytical Chemistry, Northwest University, Xi'an, Shaanxi 710069, China
e-mail: zhengjb@nwu.edu.cn

of the nonaqueous media on the electrochemical characteristics of SmHCF [40].

Even among rare earth MHCFs, different electrochemical behaviors were observed by the same group. For example, electrochemically prepared DyHCF showed two kinds of particles that varied in size and shape [41]. Thus, considerable investigations should be carried out on the electrochemical behaviors of different rare earth MHCFs and developing new kinds of sensors which can be used in practice. We have studied the electrochemical behavior of neodymium hexacyanoferrate (NdHCF)-modified electrodes prepared by the proposed method of mechanically attaching NdHCF to the surface of CCEs, and the resulting modified electrode showed excellent electrocatalytic ability to the reduction of hydrogen peroxide [42]. After that, the electrochemical characteristics of terbium hexacyanoferrate (TbHCF) were studied as well [43]. As a continuation of our research work, the electrochemical characteristics of another rare earth MHCFs, ErHCF, was thoroughly investigated, and L-cysteine was chosen as a model compound to elucidate the electrocatalytic ability of the ErHCF-modified CCE. Based on the strong electrocatalytic ability and good stability of the modified electrode towards L-cysteine, amperometric method was used for the determination of L-cysteine in real samples.

Materials and methods

Chemicals

Methyltrimethoxysilane (MTMOS) was purchased from Guibao chemical engineering limited company of Hangzhou. High purity graphite powder was purchased from Shanghai Carbon Plant. Erbium chloride hexahydrate (99.9%) was used without further purification. Potassium ferrocyanide [$K_4Fe(CN)_6$] and potassium chloride (KCl) were of analytical grade, and all solutions were prepared with ultrapure water obtained from a Millipore Milli-Q water purification system. The stock solutions of L-cysteine (Shanghai Biochemical Plant, Shanghai, China) were prepared immediately before use and were deaerated with purified nitrogen.

Apparatus

Fourier transform infrared (FTIR) spectrum of ErHCF was recorded on KBr disk using a Nicolet 380 FT-IR Spectrometer (Thermo Electron Corporation, USA). The iron, erbium, and potassium content of the sample are determined by inductively coupled plasma (ICP) atomic emission spectroscopy (IRIS Advantage, Thermo Jarrell Ash USA) of the digested samples. Digestion was achieved by hydrochloric acid. X-ray diffraction (XRD) experiments were performed with a Shimadzu XD-3A X-ray diffractometer (Japan) using Cu-Ka radiation (k=0.15, 418 nm). The scan rate was 4°/min. X-ray photoelectron spectroscopy (XPS) was obtained by using monochromatic Al Kα radiation (150 W, 15 kV, 1,486.6 eV), Axis Ultra, Kratos (UK). The vacuum in the spectrometer was 10^{-9} Torr. Binding energies were calibrated relative to the C1s peak (284.8 eV) from hydrocarbons adsorbed on the surface of the samples. A model CHI660A Electrochemistry Workstation (Chenhua Instruments in Shanghai, China) was employed for all the electrochemical techniques. There is a three-electrode system, where a standard saturated calomel electrode (SCE) served as reference electrode, a platinum wire electrode as the auxiliary electrode, and the ErHCF-modified electrodes as the working electrode. All the electrochemical experiments were carried out at room temperature.

Preparation of samples and electrodes

The ErHCF sample was synthesized by precipitation via dropwise addition of 50 ml of 10.0 mM $ErCl_3$ into a vigorous stirred solution of 50 ml of 10.0 mM $K_4Fe(CN)_6$ (each containing 0.5 M KCl). The resulting precipitates were collected by filtration and washed with 0.5 M KCl electrolyte and ultrapure water, respectively. The samples were dried overnight in vacuum at ambient temperature and stored in a desiccator. The bare CCEs were prepared according to the procedure described by Lev and coworkers [44]. After drying for 48 h at room temperature, the electrode was polished with polishing paper to remove extra composite material. Solid samples of ErHCF were mechanically attached to the surface of CCE according to a published report [38]. A copper wire through the back of the electrodes makes electric contacts. The surface of CCE can be renewed after each experiment by rubbing the electrode surface on a clean abrasive. As for comparison, the ErHCF-modified glassy carbon electrode (GCE) obtained by the deposition of a thin layer at a GCE surface was fabricated. The fabricating process was carried out in a 0.5 M KCl solution containing 1.0 mM $ErCl_3$, 1.0 mM $K_3Fe(CN)_6$, pH 2.0. After a series of consecutive potential cycling for 20 cycles (about 5 min), the electrode was removed from the solution and washed with water.

Result and discussion

Characterization of ErHCF and ErHCF-modified CCE

To verify the composition of the synthesized ErHCF samples, it is necessary to characterize ErHCF samples by

some techniques, such as FTIR, XRD, ICP atomic emission spectroscopy, and XPS experiments. Figure 1a is the typical FTIR spectrum of ErHCF samples. As can be seen from the spectrum, the main peaks appear at 3,585, 3,348, 2,080, 1,646, 1,597, 600, and 467 cm^{-1} are quite similar with the typical characteristic absorption peak of MHCFs, such as PB [45–47] and its analogs [48, 49]. The iron, erbium, and potassium content of the sample are determined by ICP atomic emission spectroscopy. The results show that the atomic ratio is 1:1:1, which is the same as expected with other rare earth MHCFs such as SmHCF [34], DyHCF [35], LaHCF [36], NdHCF, [42] and TbHCF [43]. These results indicate that there is only one stoichiometric compound existing in the ErHCF system.

This conclusion is also verified by the results of XRD experiment (Fig. 1b). The major peaks appeared at 16.15, 20.06, 35.61, 36.71, and 43.70, in very good agreement with the values of potassium iron erbium cyanide hydrate previously reported [$ErKFe(CN)_6 3H_2O$, JCPDS card, file 31-1002], which confirms further that the compound is a crystalline form of $ErKFe(CN)_6 3H_2O$.

XPS spectrum is also used to further identify the oxidation state of iron and erbium in ErHCF samples. From Fig. 2, the Fe 2p regions appear at 706.5 and 719.3 eV, ascribed to the characteristics of Fe(II) [50], while the Er 4d region appears at 167.1 eV, ascribed to the characteristic of Er(III) .

SEM experiments are carried out to have an intuitionistic understanding about the conformation of ErHCF samples on the electrode surface. Just as expected, the surface of a bare CCE shows porous three-dimensional structure, while in ErHCF-modified CCE, the solid ErHCF materials are entrapped into the pore network of the electrodes (Fig. 3), which was the same as reported by our previous report [42].

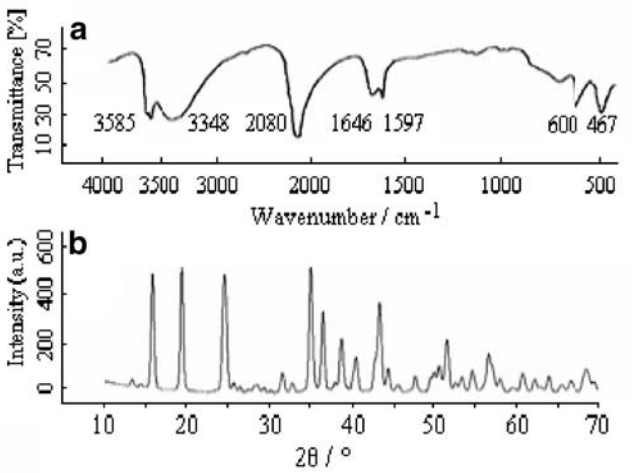

Fig. 1 FTIR spectra (**a**) and XRD pattern of ErHCF (**b**)

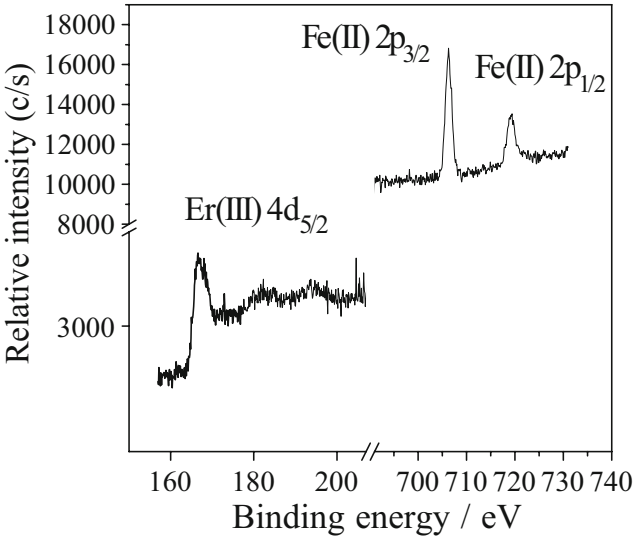

Fig. 2 XPS spectra of the Fe 2p region and Er 4d region of ErHCF

Electrochemical behavior of ErHCF-modified CCE

The investigation of the electrochemical behavior of ErHCF-modified CCE and ErHCF-modified GCE are carried out in a 0.5 M KCl (pH 7) solution. Results show that both electrodes show a pair of well-defined redox peaks with the formal potential of +0.215 V (vs SCE). The peak potentials of the two electrodes are almost the same, which suggest that only one stoichiometric compound exist in both systems. However, the peak currents of the ErHCF-modified GCE decrease rapidly with the increase in the scan numbers. In fact, only 65% of the initial one after 100 repeated scans is observed. This is the main reason that we chose CCE for the fabrication of ErHCF-modified electrode and which was subsequently used for the determination of L-cysteine. The formal potential of ErHCF-modified CCE is very close to that of other rare earth MHCFs [34–36, 42, 43], but is more negative than that of transition MHCFs, such as CoHCF [20] and NiHCF [21]. Figure 4 is the cyclic voltammograms of the ErHCF-modified CCE obtained in 0.5 M KCl (pH 7) at various scan rates. The values of ΔE_p are almost independent on the scan rates in the range of 10–00 mV s^{-1}. Inset graph of Fig. 4 shows that the cathodic and anodic peak currents increase linearly with the increase of square root rates, suggesting that the electrochemical reaction of ErHCF-modified CCE is not a surface-controlled process but a diffusion-controlled one at the time of reaching the peak potential [49]. Here, it is necessary to mention that it is indeed only the diffusion of K^+ in the ErHCF lattice, and not in the solution, which can be rate determining when the solution concentration is 0.5 M, and the bulk diffusion is not rate determined. Also, the peak current increased with the increase in K^+ concentration, suggesting that the concentration of K^+ in ErHCF crystal is not high enough, and the diffusion of K^+

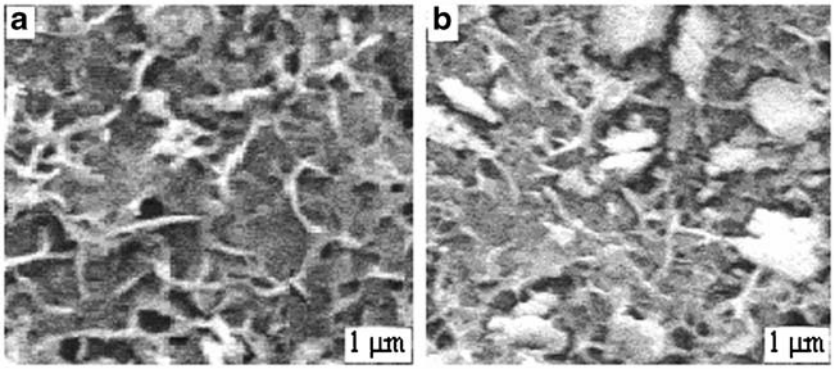

Fig. 3 SEM images of the surfaces of **a** bare CCE and **b** ErHCF-modified CCE

in ErHCF crystal cannot be neglected. Quantificationally, from the relationship between the peak current and the concentration of K^+, the value of peak current is related to the concentration of K^+. Here, the partition coefficient of K^+ at the crystal/solution interface will not be influenced by the changes of K^+ concentration, which guarantee that the concentration of K^+ in ErHCF crystal is proportional to the concentration of K^+ in solution. The results of transport of ions and electrons during electrochemical reactions have been confirmed by Moon et al. [51] and described as electrolytic conduction, whereas on the CCE, the ErHCF is surrounded by the aqueous electrolyte, with which cations are exchanged; in the case of the CCEs, it is in a hydrophobic environment. In the presence of water, the counterions form a cloud called the double layer around the ErHCF particle. This phenomena is the same as in the case of PB [52] and other rare earth MHCFs [34–36, 42, 43]. Kulesza et al. [53] also verified the insertion of a counterion into the film during the reduction and its exclusion upon oxidation by using the electrochemical quartz crystal microbalance technique.

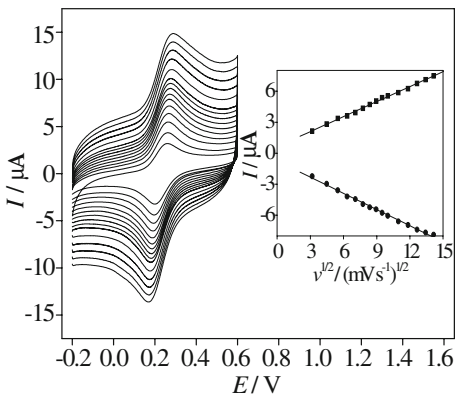

Fig. 4 Cyclic voltammograms of the ErHCF-modified CCE in 0.5 M KCl (pH 7) solution at various scan rates (from inner to outer curve): 10, 20, 30, 40, 50, 60, 70, 80, 90, 100, 120, 140, 160, 180, and 200 mV s^{-1}; Inset graphs: plots of peak currents vs square root of scan rates

At higher scan rates wherein $v \geq 200$ mV s^{-1}, both the anodic and cathodic peak potentials move towards the negative direction, and the peak separation (ΔE_p) begins to increase with the increase of scan rates, which indicated the limitation arising from charge transfer kinetics. The values of anodic and cathodic peak potentials ($E_{p,a}$ and $E_{p,c}$) are proportional to the logarithm of the scan rate for $v \geq$ 1,000 mV s^{-1}. Based on the Laviron theory [54], the electron transfer rate constant (k_s) and the transfer coefficient (α) can be calculated. For cathodic and anodic peaks, the slope of E_p ($E_{p,a}$ and $E_{p,c}$) vs. log v is −0.1868 and 0.2421, respectively. The calculated value of α is 0.48. According to the following equation:

$$\log k_s = \alpha \log(1-\alpha) + (1-\alpha)\log\alpha - \log (\mathrm{RT}/nFv) - \alpha(1-\alpha)nF\Delta E_p/2.3\mathrm{RT} \quad (1)$$

The calculated value of k_s and α is about 1.9 s^{-1} and 0.48, respectively.

Similar to other MHCFs, the voltammetric behavior of the ErHCF-modified CCE is highly dependent on the concentration of the alkali metal ions. Furthermore, the peak current increased with the increase in K^+ concentration. According to the discussion made on the thermodynamic behavior for the redox system of PB and its analogues described by Itaya et al. [55], the alkali metal

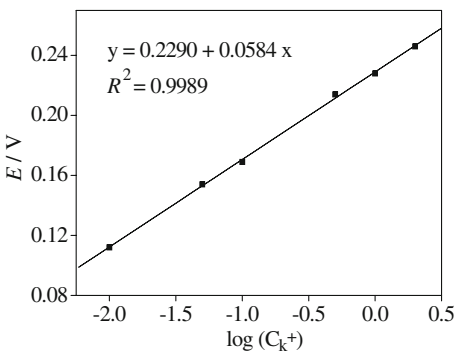

Fig. 5 Plots of E vs log (C_{K+})

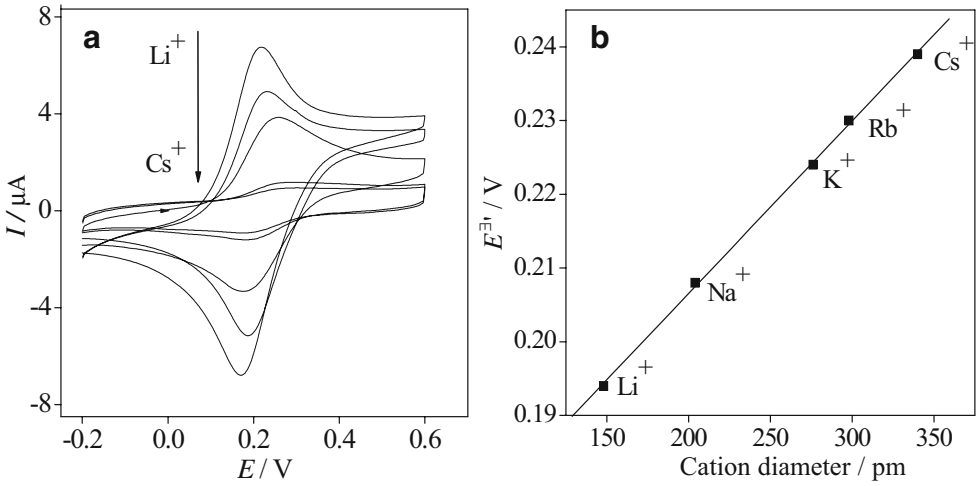

Fig. 6 **a** Cyclic voltammograms of the ErHCF-modified CCE in the presence of different alkali metal cation chloride supporting electrolytes with the same concentration (0.5 M); scan rate: 50 mV s^{-1}; **b** Plot of $E_c^{\ominus'}$ vs cation diameter of alkali metals

ion of the supporting electrolyte is involved in the redox reaction of the electroactive material. Based on the Nernst equation:

$$E = E_c^{\ominus'} + \mathrm{RT}/F \ln[\mathrm{ErHCF}][\mathrm{M}^+]/[\mathrm{ErMHCF}] \quad (2)$$

where [ErHCF] and [ErMHCF] refer to the concentration of ErHCF and its alkali metal salt respectively, and $E_c^{\ominus'}$ is the formal potential of the system. Figure 5 shows the plot of peak potential vs log (C_{K+}) for the modified electrode in KCl solutions. The curve has a slope of 58.4 mV per decade, which is close to the theoretical Nernst response of 59 mV per decade. Therefore, the electrode reaction process of the redox couple can be expressed as follows:

$$\mathrm{KErFe^{II}(CN)_6} \rightleftarrows \mathrm{ErFe^{III}(CN)_6} + \mathrm{K^+} + \mathrm{e^-} \quad (3)$$

Another important characteristic of MHCF-type modified electrodes is that the type of cation of the supporting electrolyte affects the electrochemical behavior of the electrodes. First, different shapes of the cyclic voltammograms can be obtained in the presence of different cations, which can be explained partly by the assumption that an enthalpy term must be included in the free energy, as has been described for PB [56]. Secondly, another main effect is that the peak potential of the MHCF-modified electrode changes with the type of cations of the supporting electrolyte. Those effects are also observable for the system under investigation. From Fig. 6, the peak potential for redox couple shifts slightly to more positive potential by increasing the cations' diameter, which is the same as other rare earth MHCFs reported before [34–36, 42, 43]. The peak currents of the ErHCF-modified CCE decrease in the order of Li^+, Na^+, K^+, Rb^+, and Cs^+ in the same concentration of electrolyte solution, suggesting that the permeability of cations of the ErHCF-modified CCE in different supporting electrolytes is: $Li^+ > Na^+ > K^+ > Rb^+ > Cs^+$.

Electrocatalysis of L-cysteine

L-cysteine, a sulfur-containing amino acid which appears in structures of peptides and proteins, plays a crucial role in living systems. Therefore, the determination of L-cysteine is very important from either the biological or pharmacological standpoints. CMEs for the detection of L-cysteine have attracted considerable interests because of their high sensitivity, simplicity, and feasibility to the development in vivo sensors and chromatographic detectors [57, 58]. Figure 7 shows the cyclic voltamograms for the ErHCF-

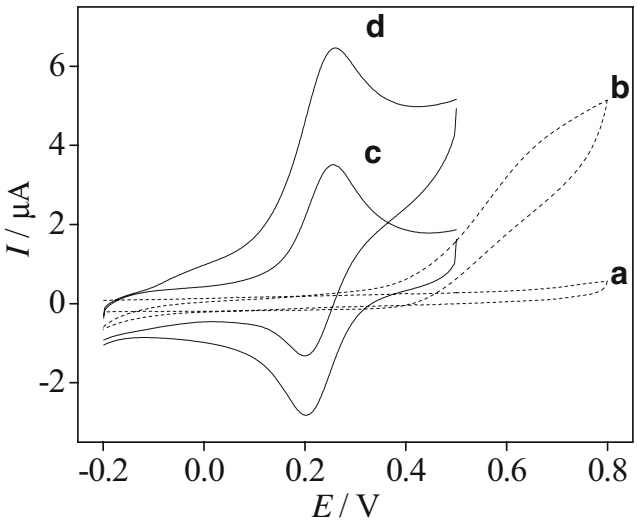

Fig. 7 Cyclic voltammograms of a bare CCE (*dash line*) and ErHCF-modified CCE (*solid line*) in 0.5 M KCl (pH 7) solution at a scan rate of 20 mV s^{-1}: In the absence (*a*, *c*), and presence (*b*, *d*) of 0.5 mM L-cysteine

modified CCE in the presence and absence of 0.5 mM L-cysteine. As can be seen, the anodic peak current increases noticeably, and the cathodic peak current decrease after addition of 0.5 mM L-cysteine, while at the bare CCE, L-cysteine is not oxidized until +0.6 V. It is necessary to mention that this kind of electrode decreases the overpotential about 400 mV for L-cysteine oxidation dramatically, compared with other kinds of electrodes modified with Ru complex [59] and MnHCF [19]. This decrease in overpotential and enhancement of peak current for L-cysteine oxidation indicates a catalytic effect of the ErHCF-modified CCE.

Electrolyte pH and applied potential study

The effect of pH of the supporting electrolyte on electrocatalytic oxidation of L-cysteine is evaluated. Results show that there are no obvious changes in the electrocatalytic behavior in the pH range of 4–8. However, the catalytic current becomes smaller when the pH of the supporting electrolyte is out of the range. The possible reason may be due to the dissolution of the mediator in both acidic and basic conditions. Thus, 0.5 M KCl (pH 7) is selected as electrolyte throughout the experiments.

Figure 8 shows the hydrodynamic voltammetric *I–E* curves obtained at the bare CCE and ErHCF-modified CCE for injections of 0.5 mM L-cysteine in a stirred 0.5 M KCl (pH 7) solution. These data were plotted as a function of applied potential to obtain hydrodynamic voltammograms (relationship between the detected peak current, I_p and the applied potential E_d). Such a choice will offer maximum sensitivity and selectivity. As can be seen, the peak current reaches a maximum at +0.28 V for the electrocatalytic oxidation of L-cysteine. In contrast, the bare CCE for the electrocatalytic oxidation of L-cysteine only occurred at higher potential and with lesser sensitivity. The results are similar to that of cyclic voltammetric curves described in Fig. 6. Thus, a potential of +0.28 V is applied during the amperometric determination of L-cysteine.

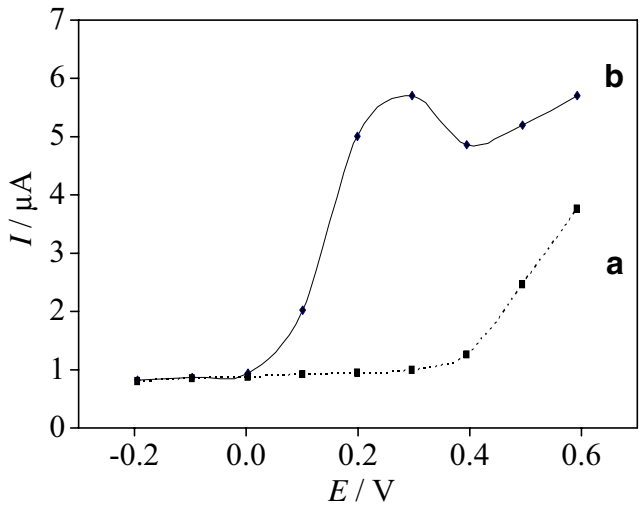

Fig. 8 Hydrodynamic voltammograms for the oxidation of 0.5 mM L-cysteine at a bare CCE (*a*) and ErHCF-modified CCE (*b*) in 0.5 M KCl (pH 7) solution

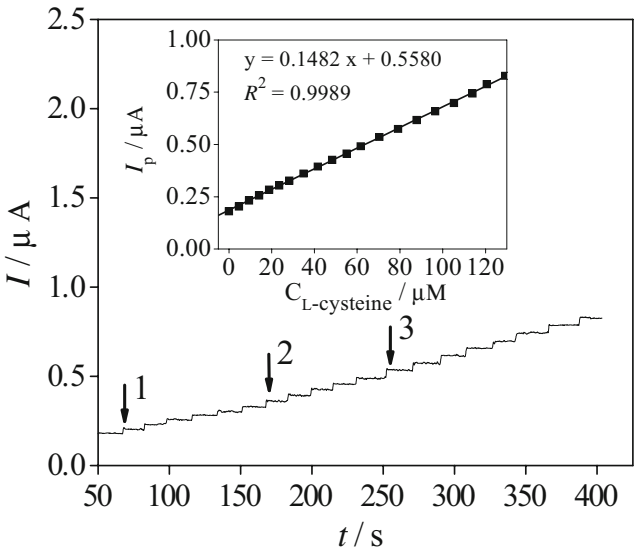

Fig. 9 Amperometric response observed at ErHCF-modified CCE during successive addition of *1* 50.0, *2* 75.0, and *3* 100.0 μl 1.0 mM L-cysteine into a continuously stirred 10.0 ml 0.5 M KCl (pH 7) solution. Applied potential: +0.28 V. *Inset graphs*: plot of chronoamperometric currents vs L-cysteine concentration

Amperometric detection of L-cysteine at ErHCF-modified CCE

Based on the voltammetric results described above, amperometric current–time response is recorded to estimate the detection limit and the calibration curve for L-cysteine detection at the ErHCF-modified CCE. Figure 9 shows the typical L-cysteine amperograms during the successive addition of 50.0, 75.0, and 100.0 μl 1.0 mM L-cysteine into a continuously stirred 10.0 ml 0.5 M KCl (pH 7) solution, under conditions which the potential of modified electrode is kept at +0.28 V. As can be seen, a well-defined response is observed on the graph. The calibration plot for L-cysteine determination is linear at 5.0×10^{-6}–1.3×10^{-4} M with a linear regression equation of $I(A) = 0.558+0.148c$ (μM) ($R^2 = 0.9989$, $n = 20$), and the detection limit is 2×10^{-6} M ($S/N = 3$).

Stability and reproducibility

The stability of ErHCF-modified CCE is first checked by recording the cyclic voltammograms during 10 h with a time scale of 1 h in 0.5 M KCl (pH 7) solution. Results

show that the current responses of the electrode are almost the same within 10 h. The electrochemical and electrocatalytic storage stability of the modified electrode is further evaluated within 2 months by recording the current responses once each day. Results show that the electrocatalytic ability of the modified electrodes remain almost the same as the initiate one after 2 months. Those results indicate that the solid state voltammetric characteristics and the electrocatalytic ability of ErHCF is fairly stable. We think that the good stability of the ErHCF-modified CCE is related to the chemical and mechanical stability of the silicate matrix, the limited wetting section controlled by methyl group, especially high capacity for physically entrapping solid electroactive materials into the pores of the silicon–carbon network of electrodes, which has been illustrated in our previous work [42].

Series of replicate addition of 1.0 mM L-cysteine into a 0.5 M KCl (pH 7) solution are recorded for evaluating reproducibility of ErHCF-modified CCE for L-cysteine detection. Indeed, the responding currents of the ErHCF-modified CCE towards L-cysteine oxidation are almost the same as of its initial one and the relative deviation (n=10) is less than 5.0%. Also, after rising with water, the current response of the modified electrode returns to its initial state after the measurement. Thus, the ErHCF-modified CCE is found to exhibit good stability and reproducibility for L-cysteine detection.

Interference study and real sample analyses

The possible interference of foreign matters, which might occur in real samples, is tested. The results are shown in Table 1. When the concentrations of Ca^{2+}, Mg^{2+}, phosphate, urea, glucose, and glycin coexisting in the sample are 20 times that of L-cysteine, no significant interference could be observed, indicating that these species do not affect the determination of L-cysteine. However, ascorbic acid (AA) and Fe^{3+} might be main interferences to ErHCF-modified CCE for the electrocatalytic oxidation of L-cysteine. When the concentration of AA and Fe^{3+} are five times that of L-cysteine, the peak currents show an increase of approximately 20 and 15%, respectively. The reason may be that the oxidation of AA also occurred in the same potential range. As for Fe^{3+}, there is no current rise that can be observed without the addition of L-cysteine. However, the current response increases when Fe^{3+} coexists in the solution, which may be due to the fact that Fe^{3+} can catalyze the oxidation of L-cysteine.

Table 1 Interference effects of external matters to detection of 50 μM L-cysteine to ErHCF-modified CCE in 0.5 M KCl solution (pH 7)

External matters	Concentration spiked (mM)	Response change (%)	Relative standard deviation (n=5) (%)
Mg^{2+}	0.1	2.3	1.2
Ca^{2+}	0.1	5.1	2.5
Phosphate	0.1	−4.6	2.8
Urea	0.1	−0.5	1.9
Glucose	0.1	1.9	2.0
Glycin	0.1	8.4	2.0
Fe^{3+}	0.025	14.8	3.9
AA	0.025	20.1	2.8

Table 2 Results of the determination of L-cysteine in the presence of human urine

Sample	Added (μM)	Found (μM)[a]	Recovery (%)
Human urine	10	9.85	98.5
	20	20.3	101.5
	50	48.6	97.2
	100	99.4	99.4

[a] The average value of three measurements

As a practical use, ErHCF-modified CCE is also used to detect L-cysteine in the presence of human urine (nature). The urine samples, obtained from healthy volunteers, are detected directly without the need of pretreatment or adding other reagents. Every 1 ml of fresh sample is taken and diluted to 10 ml with water before the detection. The recoveries of L-cysteine are determined by standard addition, and the corresponding results are given in Table 2. The recovery for four samples is found to be in the range of 97.2–101.5%. This result suggests that ErHCF-modified CCEs are very reliable and sensitive with regard to determining L-cysteine.

Conclusions

We have demonstrated a kind of ErHCF-modified CCE prepared by mechanically attaching ErHCF samples to the surface of CCEs. The ErHCF-modified CCE exhibited excellent electrocatalytic ability towards L-cysteine with a marked decrease in the overvoltage about 400 mV for L-cysteine oxidation, compared with the bare CCE. In addition, the present electrodes have the advantages of easy preparation, surface renewal, bulk modification, and good stability, which provide efficient probabilities for developing sensitive sensors for the detection of L-cysteine in real samples.

Acknowledgement The authors gratefully acknowledge the financial support of this project by the National Science Foundation of China (No. 20675062) and the Natural Science Foundation of Shaanxi Province of China (No.2004B20).

References

1. Murray RW (1992) In: Murray RW (ed) Molecular design of electrode surfaces, techniques of chemistry series, vol 22. Wiley, Chichester, pp 49–118
2. Zadronecki M, Linek IA, Stroka J, Wrona PK, Galus Z (2001) J Electrochem Soc 148:348
3. Jeerage KM, Steen WA, Schwartz DT (2002) Chem Mater 14:530
4. Vittal R, Jayalakshmi M, Gomathi H, Rao GP (1999) J Electrochem Soc 146:786
5. Carpenter MK, Conell RS, Simko SJ (1990) Inorg Chem 29:845
6. Kulesza PJ, Malik MA, Miecznikowski K, Wolkiewicz A, Zamponi S, Berrettoni M, Marassi R (1996) J Electrochem Soc 143:10
7. Kaneko M, Okada T (1988) J Electroanal Chem 255:45
8. Kalwellis-Mohn S, Grabner EW (1989) Electrochim Acta 34:1265
9. Jayalakshmi M, Scholz F (2000) J Power Sources 91:217
10. Nishizawa M, Kuwabata S, Yoneyama H (1996) J Electrochem Soc 143:3462
11. Wu Y, Pfenning BW, Bocarsly AB (1995) Inorg Chem 34:4262
12. Sawant SN, Bagkar N, Subramanian H, Yakhmi JV (2004) Philos Mag 84:2127
13. Casero E, Pariente F, Lorenzo E (2003) Anal Bioanal Chem 375:294
14. Tsiafoulis CG, Trikalitis PN, Prodromidis MI (2005) Electrochem Commun 7:1398
15. Neff VD (1978) J Electrochem Soc 125:886
16. Itaya K, Ataka T, Toshima S (1982) J Am Chem Soc 104:3751
17. Eftekhari A (2003) J Power Sources 117:249
18. Gao ZQ (1994) J Electroanal Chem 370:95
19. Wang P, Jing XY, Zhang WY, Zhu GY (2001) J Solid State Electrochem 5:369
20. Liu MC, Li P, Zhang L, Xian YZ, Ding HC, Zhang CL, Zhang FF, Jin LT (2005) Chin J Chem 23:983
21. Wang P, Yuan Y, Jing XY, Zhu GY (2001) Talanta 53:863
22. Liu YQ, Yan Y, Shen HX (2005) Chin J Chem 23:1165
23. Mullica DF, Perkins HO, Sappenfield EL, Leschnitzer D (1989) Acta Crystallogr C 45:330
24. Petter W, Gramlich V, Hulliger F (1989) J Solid State Chem 82:161
25. Grallagher PK, Prescott B (1970) Inorg Chem 9:2510
26. Sakamoto M, Matsuki K, Ohsumi R, Nakayama Y, Matsumoto A, Okawa H (1992) Bull Chem Soc Jpn 65:2278
27. Mullica DF, Perkins HO, Sappenfield EL, Grossie DA (1988) J Solid State Chem 74:9
28. Willems JJG (1984) Philips J Res 39:1
29. Van Druten GMR, Labbé E, Paul-Boncour V, Périchon J, Percheron-Guéau A (2000) J Electroanal Chem 487:31
30. Zhao S, Sin JKO, Xu B, Zhao M, Peng Z, Cai H (2000) Sens Actuators, B 64:83
31. Scholz F, Meyer B (1998) In: Bard AJ, Rubinstein I (eds) Voltammetry of solid microparticles immobilized on electrode surfaces in electroanalytical chemistry, vol 20. Marcel Dekker, New York, p 1
32. Liu SQ, Chen HY (2002) J Electroanal Chem 528:190
33. Zakharchuk NF, Naumov N, Stösser R, Schröder U, Scholz F, Mehner H (1999) J Solid State Electrochem 3:264
34. Wu P, Cai CX (2005) Chin J Chem 23:127
35. Wu P, Cai CX (2005) Electroanalysis 17:1583
36. Wu P, Cai CX (2004) J Solid State Eletrochem 8:538
37. Scholz F, Lange B (1992) Trends Anal Chem 11:359
38. Dostal A, Meyer B, Scholz F, Schröder U, Bond AM, Marken F, Shaw SJ (1995) J Phys Chem 99:2096
39. Wu P, Cai CX, Lu TH (2004) Chin J Appl Chem 11:25
40. Wu P, Cai CX (2005) J Electroanal Chem 576:49
41. Wu P, Shi YM, Cai CX (2006) J Solid State Electrochem 10:270
42. Sheng QL, Yu H, Zheng JB (2007) Electrochim Acta 52:4506
43. Sheng QL, Yu H, Zheng JB (2007) J Electroanal Chem 606:39
44. Tsionsky M, Gun J, Glezer V, Lev O (1994) Anal Chem 66:1747
45. Ogura K, Nakayama M, Nakaoka K (1999) J Electroanal Chem 474:101
46. Kulesza PJ, Zamponi S, Berrettoni M, Marassi R, Malik MA (1995) Electrochim Acta 40:681
47. Vittal R, Gomathi H (2002) J Phys Chem B 106:10135
48. Sinha S, Humphrey BD, Bocarsly AB (1984) Inorg Chem 23:203
49. Ayers JB, Piggs WH (1971) J Inorg Nucl Chem 33:721
50. Vannerberg NG (1976) Chem Scr 9:122
51. Moon SB, Xidis A, Neff VD (1993) J Phys Chem 97:1634
52. Zakharchuk NF, Meyer B, Henning H, Scholz F, Jaworksi A, Stojek Z (1995) J Electroanal Chem 398:23
53. Kulesza PJ, Malik MA, Berrettoni M, Giorgetti M, Zamponi S, Schmidt R, Marassi R (1998) J Phys Chem B 102:1870
54. Laviron E (1979) J Electroanal Chem 101:19
55. Itaya K, Uchida I, Neff VD (1986) Acc Chem Res 19:162
56. McCarger JW, Neff VD (1988) J Phys Chem 92:3598
57. Halbert MK, Baldwin RP (1985) Anal Chem 57:591
58. Shi G, Lu J, Xu F, Sun W, Jin L, Yamamoto K, Tao S, Jin J (1999) Anal Chim Acta 391:307
59. Salimi A, Hallaj R, Amini MK (2005) Anal Chim Acta 534:335